Digital subcarrier multiplexing for fiber nonlinearity mitigation in coherent optical communication systems

Meng Qiu,[1,*] Qunbi Zhuge,[1] Mathieu Chagnon,[1] Yuliang Gao,[1,2] Xian Xu,[1] Mohamed Morsy-Osman,[1] and David V. Plant[1]

[1]*Department of Electrical and Computer Engineering, McGill University, Montreal, QC, H3A 2A7, Canada*
[2]*Photonics Research Centre, Department of Electrical Engineering, The Hong Kong Polytechnic University, Hong Kong, China*
[*]*meng.qiu@mail.mcgill.ca*

Abstract: In this work we experimentally investigate the improved intra-channel fiber nonlinearity tolerance of digital subcarrier multiplexed (SCM) signals in a single-channel coherent optical transmission system. The digital signal processing (DSP) for the generation and reception of the SCM signals is described. We show experimentally that the SCM signal with a nearly-optimum number of subcarriers can extend the maximum reach by 23% in a 24 GBaud DP-QPSK transmission with a BER threshold of 3.8×10^{-3} and by 8% in a 24 GBaud DP-16-QAM transmission with a BER threshold of 2×10^{-2}. Moreover, we show by simulations that the improved performance of SCM signals is observed over a wide range of baud rates, further indicating the merits of SCM signals in baud-rate flexible agile transmissions and future high-speed optical transport systems.

OCIS codes: (060.1660) Coherent communications; (060.2330) Fiber optics communications.

References and links

1. E. Ip and J. M. Kahn, "Compensation of dispersion and nonlinear impairments using digital backpropagation," J. Lightwave Technol. **26**(20), 3416–3425 (2008).
2. L. B. Du and A. J. Lowery, "Improved single channel backpropagation for intra-channel fiber nonlinearity compensation in long-haul optical communication systems," Opt. Express **18**(16), 17075–17088 (2010).
3. E. F. Mateo, X. Zhou, and G. Li, "Improved digital backward propagation for the compensation of inter-channel nonlinear effects in polarization-multiplexed WDM systems," Opt. Express **19**(2), 570–583 (2011).
4. Z. Tao, L. Dou, W. Yan, L. Li, T. Hoshida, and J. C. Rasmussen, "Multiplier-free intrachannel nonlinearity compensating algorithm operating at symbol rate," J. Lightwave Technol. **29**(17), 2570–2576 (2011).
5. Y. Gao, A. S. Karar, J. C. Cartledge, S. S.-H. Yam, M. O'Sullivan, C. Laperle, A. Borowiec, and K. Roberts, "Simplified nonlinearity pre-compensation using a modified summation criteria and non-uniform power profile," in *Proc. OFC* (2014), paper Tu3A.6.
6. Q. Zhuge, M. Reimer, A. Borowiec, M. O'Sullivan, and D. Plant, "Aggressive quantization on perturbation coefficients for nonlinear pre-distortion," in *Proc. OFC* (2014), paper Th4D.7.
7. N. Stojanovic, Y. Huang, F. N. Hauske, Y. Fang, M. Chen, C. Xie, and Q. Xiong, "MLSE-based nonlinearity mitigation for WDM 112 Gbit/s PDM-QPSK transmission with digital coherent receiver," in *Proc. Opt. Commun. Conf.* (2011), paper OWW6.
8. B. Châtelain, C. Laperle, K. Roberts, M. Chagnon, X. Xu, A. Borowiec, F. Gagnon, and D. V. Plant, "A family of Nyquist pulses for coherent optical communications," Opt. Express **20**(8), 8397–8416 (2012).
9. X. Xu, B. Châtelain, Q. Zhuge, M. Morsy-Osman, M. Chagnon, M. Qiu, and D. Plant, "Frequency domain M-shaped pulse for SPM nonlinearity mitigation in coherent optical communications," in *Proc. OFC* (2013), paper JTh2A.38.
10. L. B. Du and A. J. Lowery, "Optimizing the subcarrier granularity of coherent optical communications systems," Opt. Express **19**(9), 8079–8084 (2011).
11. A. Bononi, N. Rossi, and P. Serena, "Performance dependence on channel baud-rate of coherent single-carrier WDM systems," in *Proc. ECOC* (2013), paper Th.1.D.5.
12. W. Shieh and Y. Tang, "Ultrahigh-speed signal transmission over nonlinear and dispersive fiber optic channel: the multicarrier advantage," IEEE Photon. J. **2**(3), 276–283 (2010).

#212243 - $15.00 USD Received 19 May 2014; revised 7 Jul 2014; accepted 9 Jul 2014; published 25 Jul 2014

13. Y. Tang, W. Shieh, and B. S. Krongold, "DFT-spread OFDM for fiber nonlinearity mitigation," IEEE Photon. Technol. Lett. **22**(16), 1250–1252 (2010).
14. Q. Zhuge, B. Chatelain, and D. Plant, "Comparison of intra-channel nonlinearity tolerance between reduced-guard-interval CO-OFDM systems and Nyquist single carrier systems," in *Proc. OFC* (2012), paper OTh1B.3.
15. Y. Zhu, J. Wang, Q. Guo, Y. Cui, C. Li, F. Zhu, and Y. Bai, "Experimental comparison of terabit Nyquist superchannel transmissions based on high and low baud rates," in *Proc. OFC* (2013), paper JW2A.37.
16. M. Qiu, Q. Zhuge, X. Xu, M. Chagnon, M. Morsy-Osman, and D. Plant, "Subcarrier multiplexing using DACs for fiber nonlinearity mitigation in coherent optical communication systems," in *Proc. OFC* (2014), paper Tu3J.2.
17. S. J. Savory, "Digital coherent optical receivers: algorithms and subsystems," IEEE J. Sel. Top. Quantum Electron. **16**(5), 1164–1179 (2010).
18. M. Oerder and H. Meyr, "Digital filter and square timing recovery," IEEE Trans. Commun. **36**(5), 605–612 (1988).
19. Q. Zhuge, M. Morsy-Osman, X. Xu, M. E. Mousa-Pasandi, M. Chagnon, Z. A. El-Sahn, and D. V. Plant, "Pilot-aided carrier phase recovery for M-QAM using superscalar parallelization based PLL," Opt. Express **20**(17), 19599–19609 (2012).
20. L. Liu, Z. Tao, W. Yan, S. Oda, T. Hoshida, and J. Rasmussen, "Initial tap setup of constant modulus algorithm for polarization de-multiplexing in optical coherent receivers," in *Proc. OFC* (2009), paper OMT2.

1. Introduction

Digital signal processing (DSP) has been widely employed in coherent optical (CO) communication systems and enables effective compensation for many types of linear impairments such as chromatic dispersion (CD) and polarization mode dispersion (PMD). However, fiber nonlinearities remain a factor that limits the achievable transmission distance in optical communication systems. In the digital domain, several methods have been proposed to mitigate the nonlinear impairments such as digital back propagation (DBP) with inverse fiber parameters [1–3], perturbation-based nonlinear pre-compensation [4–6] and maximum-likelihood sequence estimation (MLSE) [7]. However, the computational complexity of these approaches is usually high. Pulse shaping was proposed in [8, 9] as an alternative to mitigate fiber nonlinearities by increasing the power of the high-frequency components in the signal spectra. The drawback of this method is the reduced spectral efficiency (SE) because an increased bandwidth is usually required for a noticeable performance improvement.

In [10–13], it was shown by both theoretical analysis and numerical simulations that the subcarrier granularity has significant influences on the nonlinear performance of dispersion-unmanaged CO transmission systems. That means by splitting the high-baud-rate single carrier (SC) signal into multiple multiplexed low-baud-rate subcarriers and optimizing the number of subcarriers, the nonlinearity tolerance of the system can be improved even though such subcarrier multiplexed (SCM) signals generally have a higher peak-to-average power ratio (PAPR) at the beginning of the transmission link [12]. The improved nonlinearity tolerance benefitting from subcarrier multiplexing can be explained by the theory of four wave mixing efficiency [12] or the walk-off between subcarriers due to CD [14]. Similar ideas have also been demonstrated by simulations in coherent optical orthogonal frequency-division multiplexing (CO-OFDM) systems which show the reduced-guard-interval (RGI) CO-OFDM systems potentially have higher intra-channel nonlinearity tolerance than the Nyquist single carrier systems if the signal is optimized [14]. But different from CO-OFDM, each subcarrier of the SCM signal can be separated and processed independently using algorithms of single carrier systems because the spectra of subcarriers are not overlapped for SCM signals.

On the other hand, thanks to the development of high-speed digital-to-analog converters (DAC), the generation of SCM signals can be achieved readily by generating the required signals digitally in the transmitter DSP and loading the samples to DACs for digital-to-analog conversion. Since the multiplexing of subcarriers is achieved in the digital domain, the implementation penalty is expected to be smaller compared with the analog methods [15]. Therefore, digital subcarrier multiplexing also serves as a practical candidate for fiber

#212243 - $15.00 USD Received 19 May 2014; revised 7 Jul 2014; accepted 9 Jul 2014; published 25 Jul 2014

nonlinearity mitigation and a thorough experimental study of it will be instructive. In our previous work we have already demonstrated the feasibility of generating SCM signals using DACs and experimentally investigated the improved intra-channel nonlinearity tolerance of SCM signals in a 24-GBaud single-channel dual polarization (DP) quadrature phase shift keying (QPSK) transmission system [16].

In this work, we discuss in more details our work in [16]. The optimum design of SCM signals is also investigated. Moreover, we extend our study to 16-QAM transmissions and demonstrate the advantage of SCM signals in more schemes. The remainder of the paper is organized as follows. In Section 2 we introduce the transmitter and receiver DSP for the multiplexing and de-multiplexing of subcarriers. Then in Section 3, we numerically and experimentally compare the transmission properties of SC signals and SCM signals for QPSK and 16-QAM, showing that properly designed SCM signals outperform SC signals in terms of intra-channel nonlinearity tolerance. Finally we conclude in Section 4.

2. Subcarrier multiplexing and de-multiplexing

Figure 1 illustrates the simulated transmitter-side spectra of the SC signal and the SCM signals with 2, 4 and 8 subcarriers. The total baud rate is 24 GBaud, so the baud rate of each subcarrier is 12 GBaud, 6 GBaud and 3 GBaud respectively for the three SCM signals. The modulation format is QPSK. Root raised cosine (RRC) pulse shaping with a roll-off factor of 0.1 is used in this work. Note that no guard band is left between subcarriers in the SCM signal spectra, so the optical bandwidth and SE are the same for all signals.

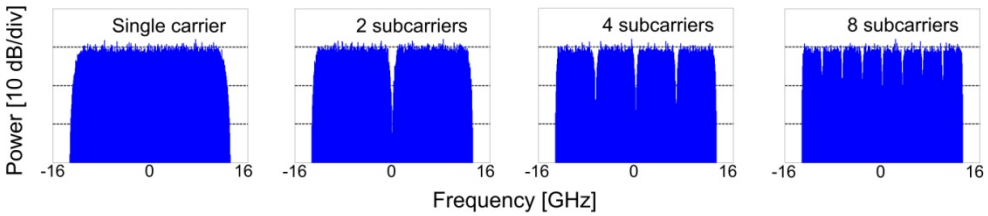

Fig. 1. Power spectra of the SC signal and SCM signals.

The subcarriers are multiplexed using the configuration shown in Fig. 2(a). K denotes the number of subcarriers in the SCM signal. Note that the SC signal can be regarded as a special SCM signal when $K = 1$, so Fig. 2 applies to the SC signal as well. Independent data sequences are used in each subcarrier and mapped to QPSK or 16-QAM symbols. After the symbols are interpolated to 2 samples per symbol in each subcarrier, the samples, denoted as S_k, $k = 1,2\ldots K$, are transformed to the frequency domain and filtered by a RRC filter $H(f)$ with a roll-off factor of 0.1. Then the outputs are up-sampled by K (essentially frequency-domain zero padding), shifted to different frequencies in the spectrum and multiplexed. These operations are also done in the frequency domain. After the re-sampling to the DAC sampling rate, the signals are pre-compensated to combat the limited bandwidth of the transmitter based on the pre-measured transmitter frequency response. Finally the time-domain samples are sent to DACs for digital-to-analog conversion. Correspondingly, for subcarrier de-multiplexing, we use a configuration as shown in Fig. 2(b). The SCM signal is first digitized by analog-to-digital converters (ADC) and re-sampled to twice the total baud rate. All subcarriers are captured simultaneously in a single detection. After the transform to the frequency domain, each subcarrier is successively shifted to the baseband and filtered out using a digital low-pass matched filter $G(f)$. Finally the low-baud-rate signal in each subcarrier is down-sampled by K (essentially truncating zeros in the frequency domain to 2 samples per symbol), transformed to time domain and processed in parallel. The other DSP blocks are similar to those in conventional SC systems and are not shown in Fig. 2.

#212243 - $15.00 USD Received 19 May 2014; revised 7 Jul 2014; accepted 9 Jul 2014; published 25 Jul 2014

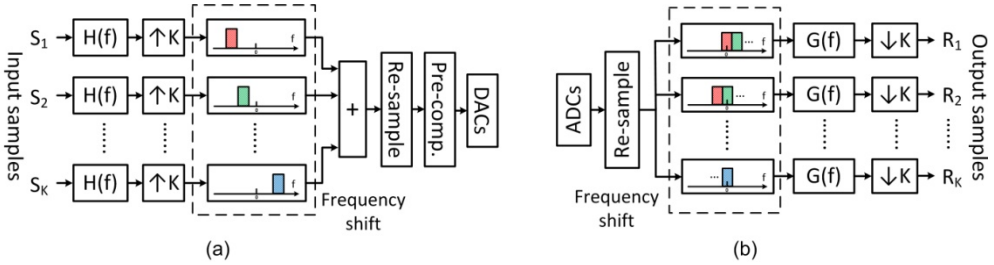

Fig. 2. Illustration of (a) the transmitter-side DSP for subcarrier multiplexing and (b) the receiver-side DSP for subcarrier de-multiplexing.

3. Setup, results and discussions

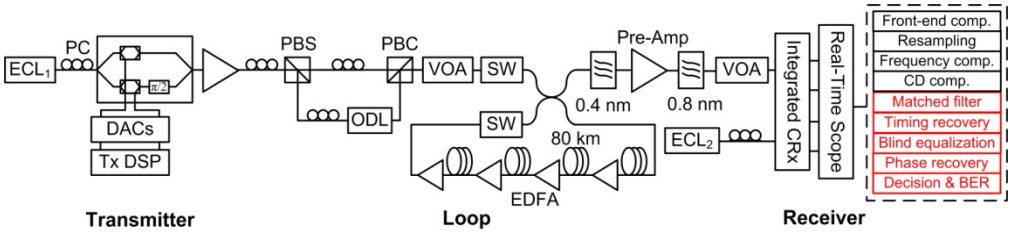

Fig. 3. Experimental setup. ECL: external cavity laser, PC: polarization controller, PBS/PBC: polarization beam splitter/combiner, ODL: optical delay line, VOA: variable optical attenuator, SW: switch, CRx: coherent receiver.

Figure 3 illustrates the experimental setup. ECLs with linewidths <100 kHz are used at both the transmitter and the receiver. The SC or SCM signals are generated offline with a total baud rate of 24 GBaud, converted to analog domain via two DACs and drive an IQ-modulator for electrical-to-optical conversion. The DACs operate at a sampling rate of 32 GSa/s with a physical resolution of 6 bits. The DP signal is emulated by splitting the signal into orthogonal polarizations and recombining them after delaying one polarization by 26 ns. This time duration corresponds to a delay of 624 symbols in the SC case. A VOA is used to control the launch power before the signals enter a re-circulating loop. The loop consists of 320 km of standard single mode fiber (SMF-28e +) and in-line EDFAs with a noise figure of 5 dB are employed after every 80 km of fiber. The output from the loop is filtered, pre-amplified and filtered again. After coherent detection by an integrated coherent receiver, the signals are digitized by a 4-channel real-time oscilloscope with a sampling rate of 80 GSa/s per channel. Finally the digital signals are processed offline in MATLAB, including IQ imbalance compensation, re-sampling, frequency offset (FO) and CD compensation [17], matched filter followed by down-sampling in the frequency domain as shown in Fig. 2(b), timing recovery [18], blind equalization and the carrier phase recovery described in [19]. For QPSK a modified version of constant modulus algorithm (CMA) [20] is used for blind equalization and for 16-QAM we use a training-symbol-aided decision-directed least mean square (DD-LMS) algorithm for better convergence with CMA for pre-convergence. A total of ~2×10^5 symbols are extracted for offline processing. The BER or Q^2 factor of the SCM signals is an average value over all subcarriers. Note that for the SCM signals the DSP blocks before matched filtering (with black color in Fig. 3) are applied to the multiplexed signal and the rest of the processing (with red color in Fig. 3) is done independently for each subcarrier.

The transmission property of different signals is first investigated numerically using MATLAB and OptiSystem. In simulations we modulate the two polarizations independently instead of using a DP emulator. Frequency offset and polarization-related transmission impairments are not considered in the simulations. The results are shown in Figs. 4(a) and 4(b) which depict the relationship between Q^2 factor and transmission distance for QPSK and

#212243 - $15.00 USD Received 19 May 2014; revised 7 Jul 2014; accepted 9 Jul 2014; published 25 Jul 2014

16-QAM transmissions respectively. The Q^2 factor here is calculated from the spread of the received constellation points after carrier phase recovery as Q^2 (in dB) = $20 \times \log_{10}(d_{min}/2\sigma)$, where d_{min} is the minimum Euclidean distance of the constellation and σ is the estimated standard deviation of the noise in the in-phase or quadrature dimension. The launch power is swept with a 1-dB step in each case and the optimum power corresponding to the maximum Q^2 factor is chosen. In both Figs. 4(a) and 4(b), it can be observed that there exists an optimum number of subcarriers, or equivalently, an optimum value of subcarrier baud rate. For example, at 3200 km in Fig. 4(a), 8 subcarriers can be considered as optimum, which means the optimum subcarrier baud rate is close to 3 GBaud in this case. In addition we note that with longer transmission distances the optimum number of subcarriers tends to increase especially for QPSK, which agrees with the simulation results in [10]. The simulation results indicate that by transmitting properly designed SCM signals instead of SC signals, the system performance can be improved significantly for both QPSK and 16QAM. To further demonstrate the improved nonlinearity tolerance of the SCM signals, we experimentally compare the performance of SC signal and SCM signals with 2, 4 and 8 subcarriers for QPSK transmissions, and SC signal and SCM signals with 2 and 4 subcarriers for 16-QAM transmissions. Note that a subcarrier number of 8 and 4 are already nearly optimum for the QPSK and 16-QAM systems respectively within the transmission range we investigate as shown in Fig. 4, so SCM signals with more subcarriers are not investigated in the following experiments.

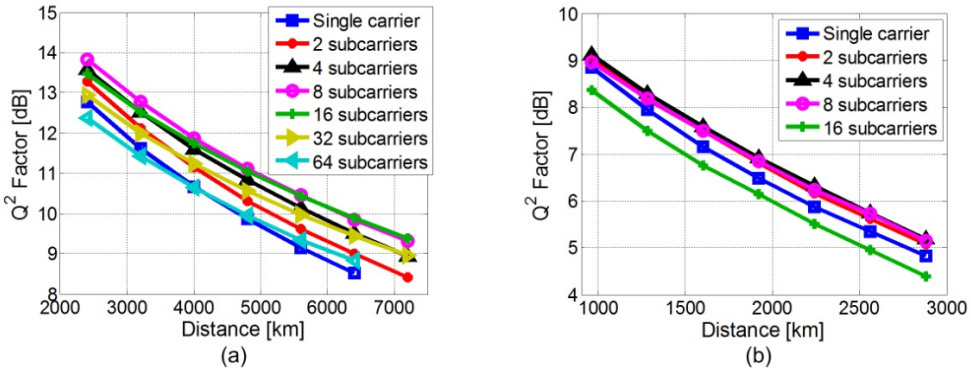

Fig. 4. Simulated Q^2 factor versus transmission distance of SC and SCM signals in a 24 GBaud (a) QPSK transmission and (b) 16-QAM transmission.

In experiments the back-to-back performance is first investigated. Figures 5(a) and 5(b) summarize the BER versus OSNR (0.1 nm) curves of different signals when the modulation format is QPSK and 16-QAM respectively. The OSNR is swept by using receiver-side noise loading and controlling the noise power using a VOA. The theoretical curves are also plotted as references. As shown in both figures, small penalties are observed when we increase the number of subcarriers. Specifically, in the QPSK case shown in Fig. 5(a), the OSNR penalty at a BER threshold of 3.8×10^{-3} is ~0.2 dB if we transmit the SCM signal with 8 subcarriers in place of the SC signal. Similarly, in the 16-QAM case in Fig. 5(b), the penalty at a BER threshold of 2×10^{-2} is ~0.3 dB if the SCM signal with 4 subcarriers is transmitted. This is because the SCM signals are more susceptible to certain types of system imperfections, e.g., the limited effective DAC resolution, the FO estimation error and the laser phase noise.

#212243 - $15.00 USD Received 19 May 2014; revised 7 Jul 2014; accepted 9 Jul 2014; published 25 Jul 2014

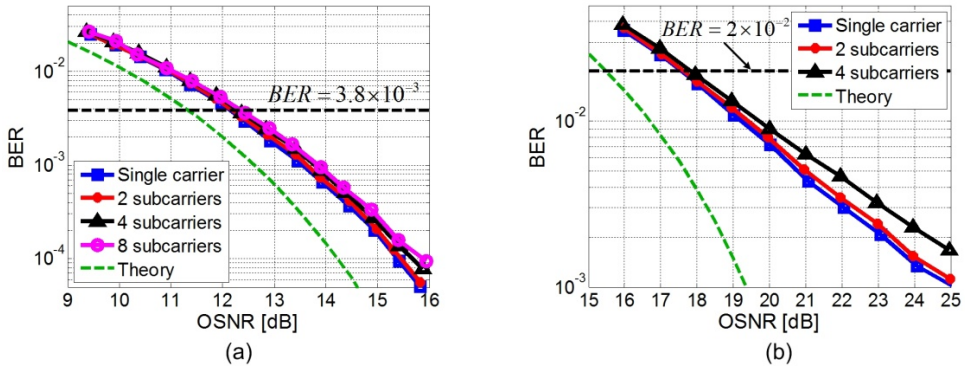

Fig. 5. Back-to-back performance of different signals with a modulation format of (a) QPSK and (b) 16-QAM.

Next we fix the transmission distance and investigate the BER under different launch powers. The results are summarized in Fig. 6(a) for QPSK transmission and in Fig. 6(b) for 16-QAM transmission. The investigated distance is 5760 km and 1920 km for these two modulation formats respectively. As shown in both figures, if the power launched into the fiber is low, e.g., –4 dBm, the systems are mainly limited by linear impairments and the BER is approximately the same for all signals. However, as the launch power increases, fiber nonlinearities become more significant. In such regimes, the SCM signals enable a lower BER than the SC signal, demonstrating the improved nonlinearity tolerance of the SCM signals. The improvement is particularly significant when the launch power is larger than –2 dBm. In terms of the optimum launch power, an increase from –2 dBm to –1 dBm is observed in the QPSK case as shown in Fig. 6(a) if the SCM signal with 8 subcarriers is transmitted instead of the SC signal. In the 16-QAM transmission, although such an increase of optimum launch power is not explicit, the better performance of the SCM signals is also observed with the optimum launch power and higher launch powers.

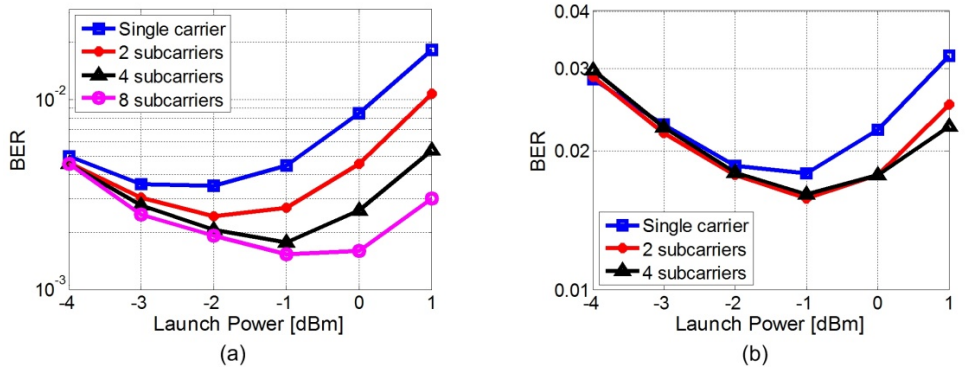

Fig. 6. BER under different launch powers in (a) QPSK transmission (at 5760 km) and (b) 16-QAM transmission (at 1920 km).

Next we compare the achievable transmission distance of different signals with a pre-set BER threshold. The results are plotted in Fig. 7(a) for QPSK transmission with a BER threshold of 3.8×10^{-3} and in Fig. 7(b) for 16-QAM transmission with a BER threshold of 2×10^{-2}. Even though we can only transmit signals for integer number of loops in the experiments, the achievable transmission distance in Fig. 7 is estimated using interpolation at the BER threshold when necessary. In accordance with the results in Fig. 6, the achievable transmission distances of different signals are similar in the linear regime with low launch powers. However, if we investigate the maximum transmission distance of different signals

#212243 - $15.00 USD Received 19 May 2014; revised 7 Jul 2014; accepted 9 Jul 2014; published 25 Jul 2014

with their respective optimum launch powers, we see that the achievable reach can be extended by transmitting the SCM signals. Specifically, in the QPSK case shown in Fig. 7(a), the optimum launch power for the SC signal is –2 dBm which enables a transmission distance of approximately 5900 km. All the three SCM signals can increase the maximum reach. In particular, the SCM signal with 8 subcarriers enables a transmission of 7250 km with its optimum power of –1 dBm. Therefore, an extension of ~23% can be achieved. In the 16-QAM case as shown in Fig. 7(b), the optimum launch power for all signals is –1 dBm, but the maximum reach is extended from 2030 km to 2200 km with this launch power if we transmit the SCM signal with 4 subcarriers in place of the SC signal. This means an extension of ~8%.

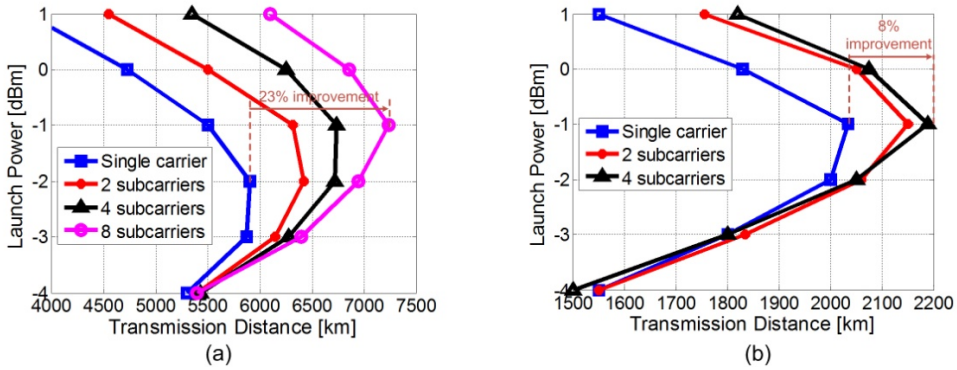

Fig. 7. Maximum transmission distance of different signals in (a) QPSK transmission with a BER threshold of 3.8×10^{-3} and (b) 16-QAM transmission with a BER threshold of 2×10^{-2}.

Finally we extend our work to other baud rates in simulations. Figure 8 shows the Q^2 factors of different signals with various total baud rates. The transmission distance is 6400 km in the QPSK case in Fig. 8(a) and 1920 km in the 16-QAM case in Fig. 8(b). The Q^2 values are obtained with the optimum launch power in each case. One thing to observe is the optimum number of subcarriers tends to increase as the total baud rate becomes larger. For example, the optimum number of subcarriers is close to 8 in the 16-GBaud QPSK system and increases to 16 when the total baud rate becomes 40 GBaud as shown in Fig. 8(a). In addition, in both figures we can see the system performance can be improved significantly within a wide range of baud rates (from 16 GBaud to 56 GBaud) by transmitting properly designed SCM signals. This result further indicates the merits of SCM signals in baud-rate flexible networks and future high-speed transmission systems.

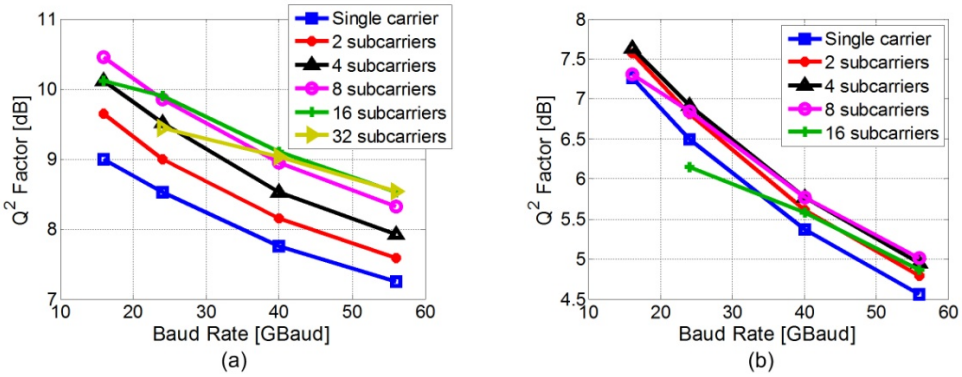

Fig. 8. Simulated Q^2 factors (with the optimum launch power) of different signals with various total baud rates (a) at 6400 km in the QPSK system and (b) at 1920 km in the 16-QAM system.

#212243 - $15.00 USD Received 19 May 2014; revised 7 Jul 2014; accepted 9 Jul 2014; published 25 Jul 2014

4. Conclusion

In this work we experimentally generate subcarrier multiplexed signals using transmitter DSP and high-speed DACs and investigate the improved intra-channel nonlinearity tolerance of the SCM signals in long-haul transmission systems. By transmitting an SCM signal with a nearly-optimum number of subcarriers, we demonstrate an extended reach of 23% for a 24-GBaud DP-QPSK system with a BER threshold of 3.8×10^{-3} and of 8% for a 24-GBaud DP-16-QAM system with a BER threshold of 2×10^{-2}. Besides, the advantage of SCM signals is demonstrated within a wide range of baud rates, which further indicates their potential applications in baud-rate adaptive transmissions and future high-speed communication systems.

#212243 - $15.00 USD Received 19 May 2014; revised 7 Jul 2014; accepted 9 Jul 2014; published 25 Jul 2014